

REMOTE SENSING FOR DIAGNOSING ACTUAL DEPLETION AND WATER USE EFFICIENCY

M. A. Bashir*, H. Tanakamaru and A. Tada

Graduate School of Agricultural Science, Kobe University, Japan

*E-mail: bashir70@yahoo.com

ABSTRACT

Monitoring the actual water depletion and water use efficiency (WUE) is critically important for water management and crop water requirements. In this paper, satellite-based energy balance model was applied to Landsat and MODIS data to quantify actual water depletion and WUE at administrative level of Gezira scheme, Sudan. The daily evapotranspiration (ET) estimated from satellite data compared well with values obtained by conventional methods. Seasonal ET (ET_s) was ranged from 30 mm to 717 mm. However, total water depletion during winter season (December 1-March 15) was $2463 \times 10^6 \text{ m}^3$. Furthermore, relations of ET_s among WUE and yield were established and discussed.

Keywords: Evapotranspiration, water use efficiency, SEBAL, Gezira scheme

1. INTRODUCTION

Actual water depletion from large irrigated areas is critically important issue for water management and crop water requirements in arid and semiarid lands. Knowledge of actual water used by agricultural crops is one of the obvious ways to save water and/or improve water use efficiency. Numerous research trials have been conducted in the Gezira scheme, Sudan to quantify ET and WUE for different crop (Farbrother [1], Fadl [2], Farah et al. [3], Salwa [4], Abdelhadi et al. [5], [6], Adeeb [7]). Despite the extensive work, the calculation of water depletion at regional-scale for long period was completely neglected. Evidence shows that point measurements found to be representative only of a relatively small area surrounding a measurement site. Also, comprehensive measurements are impossible because of the cost and difficulty. Spatial reliable information concerning ET and WUE can be used to distribute water resources and analyze the performance of irrigation systems. Remote sensing has the potential and capabilities for monitoring ET at regional scale. However, during the last decades numerous models for calculating actual ET have been developed (Menenti & Choudhury [8], Bastiaanssen [9], Kustas & Norman [10], Roerink et al. [11], Su [12], Loheide & Gorelick [13], Allen et al. [14]).

The key objectives of this paper therefore are (a) to estimate seasonal ET (ET_s) during winter season (December – March) (b) to compute and compare the total water

depletion at administrative level and (c) to estimate WUE at different administrative level to analyze irrigation performance.

2. STUDY AREA, DATA AND METHODS

The Gezira scheme is the oldest and largest gravity irrigation system in Sudan, located between the Blue and White Niles. Started in 1925 and progressively expanded thereafter, it covers about 0.9 million ha. The scheme is divided into 18 administrative units called groups; each is divided into small units called blocks. Figure 1 shows the map of the Gezira scheme with the boundaries of the 18 groups. Major crops include cotton, sorghum, groundnut and wheat (Fig. 2).

A combination of 8 MODIS images and 3 Landsat ETM+ were used in this study. The selected images were relatively cloud-free over the study area (Table 1).

Table 1. Details of MODIS and Landsat ETM+ images used

MODIS images acquisition dates		
2 December 2001		6 February 2002
11 December 2001		13 February 2002
3 January 2002		10 March 2002
21 January 2002		17 March 2002
Landsat images acquisition dates		
11 December 2001	12 January 2002	17 March 2002

Bastiaanssen et al. [15] have developed an ET algorithm called Surface Energy Balance Algorithm for Land (SEBAL). SEBAL is a single-source model, which partitions between sensible heat (H) and latent heat (LE) fluxes. It has been successfully applied in many parts of the world (Bastiaanssen [16], Trezza [17], Mohamed et al. [18], Farah et al. [19], Gao et al. [20]). The model solves the energy balance (EB) for LE as the residual (Equation 1):

$$LE = R_n - H - G \quad (1)$$

Where R_n and G are net radiation and soil heat fluxes, respectively, which are calculated based on radiometric surface temperature (T_s) and reflectance-derived values of albedo, vegetation indices (Normalized Difference Vegetation Index, NDVI), Leaf Area Index (LAI) and surface emissivity as follows:

$$R_n = R_{s\downarrow} - \alpha R_{s\downarrow} + R_{L\downarrow} - R_{L\uparrow} - (1 - \epsilon_o) R_{L\downarrow} \quad (2)$$

$$G = ((T_s - 273.15)(0.0038 + 0.0074\alpha)(1 - 0.98NDVI^4))R_n \quad (3)$$

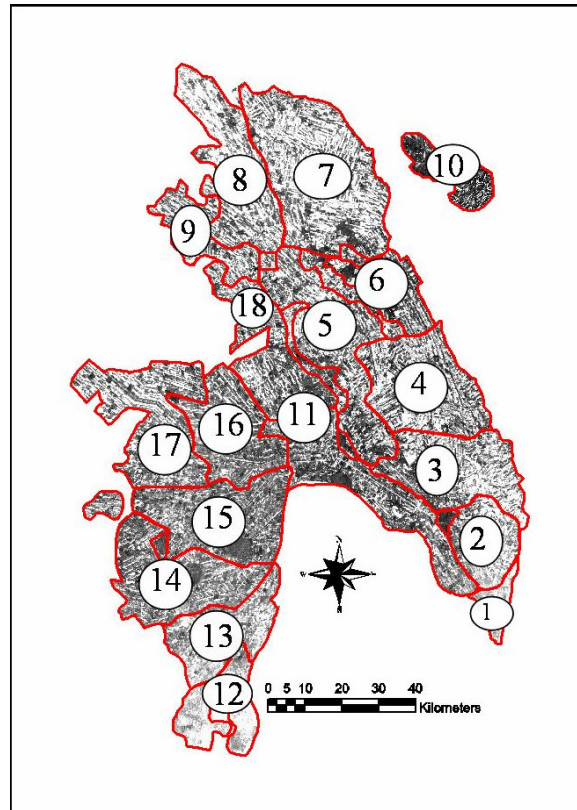


Figure 1. Gezira scheme with administrative units (1- South, 2- Hosh, 3- Center, 4- Masalamiya, 5- Wadi sha'eer, 6- Wad haboba, 7- North, 8- North West, 9- Abu Go'ta, 10- Eastern, 11- Mikashfi, 12- Shawal, 13- Gamosi, 14- Matori, 15- Ma'toug, 16- Mansi, 17- Tahameed, 18- Huda)

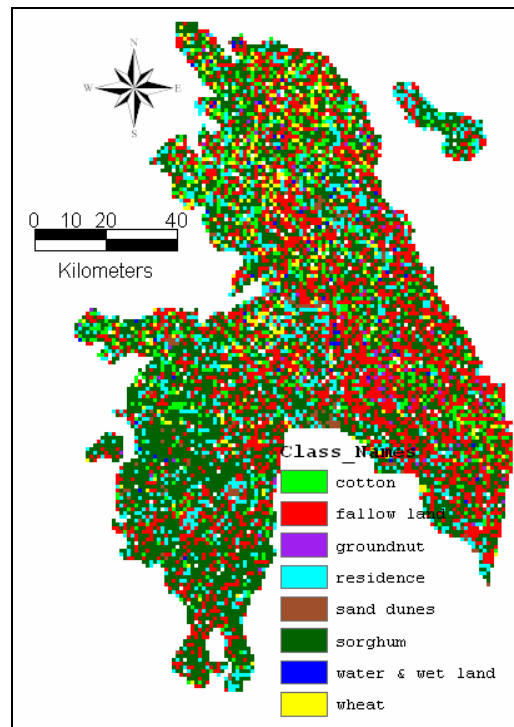


Figure 2. Land use map of the study area

where $R_{s\downarrow}$ is incoming shortwave radiation (W/m^2); α is surface albedo, $R_{L\downarrow}$ is incoming longwave radiation (W/m^2); $R_{L\uparrow}$ is the outgoing longwave thermal radiation flux emitted from the surface to the atmosphere (W/m^2); ε_o is the surface emissivity. The value of ε_o is based on soil and vegetation broad band thermal spectral emissivity (function of LAI or NDVI).

The sensible heat flux (H) is estimated using the bulk aerodynamic resistance model and a procedure that assumes a linear relationship between the aerodynamic surface temperature-air temperature difference (dT) and radiometric surface temperature (T_s) calculated from extreme pixels. Basically, extreme pixels showing cold and hot spots are selected to develop a linear relationship between dT and T_s . At the cold pixel in the image, H is assumed non-existent i.e., $H_{cold} = 0$ and at the hot pixel, LE is set to 0 which in turn allows to set $H_{hot} = (Rn - G)_{hot}$. Then, $dT_{cold} = 0$ and dT_{hot} can be obtained by solving the bulk aerodynamic resistance equation for the hot pixel as:

$$H = \rho_a C_p \frac{dT}{r_{ah}} \quad (4)$$

where ρ_a is the air density (kg/m^3), C_p is the specific heat capacity of air ($\approx 1004 \text{ J/kg/k}$); and r_{ah} is the aerodynamic resistance to heat transfer (s/m).

After calculating dT at both cold and hot pixels, a linear relationship between dT and T_s is developed to estimate H iteratively correcting r_{ah} for atmospheric stability. This is done applying the Monin-Obhukov Stability (MOS) theory. This step requires air temperature (T_a) and wind velocity (u) measured at a weather station and a mechanism that extrapolates wind speed to a blending height of 100-200 m. The dT artifice is expected to compensate for errors in surface temperature estimates due to atmospheric correction, and does not assume that radiometric and aerodynamic temperature are equivalent.

After having computed the Rn , G and H , the LE can be obtained as the residual of the energy balance equation. Assuming the evaporative fraction (Λ) to be nearly constant during the day time, the daily actual ET can be estimated from daily net radiation $Rn_{24 \text{ hours}}$ and Λ as follows:

$$\Lambda = \frac{LE}{LE + H} = \frac{Rn - G - H}{Rn - G} \quad (5)$$

$$ET = \frac{8.64 \times 10^7}{\lambda} \Lambda \times Rn_{24 \text{ hours}} \quad (6)$$

ET seasonal (ET_s) was calculated spatially following the method described by Tasumi & Allen [21]. The ET_s estimated by MODIS images at 1km was downscaled to 30 m using three Landsat ETM+ images during the season as explained by Zwart & Bastiaanssen [22]:

$$ET_s = \sum_{i=1}^{i=3} \left\{ \overline{ET_{MODIS,i}} \times \frac{ET_{Landsat,j}}{\overline{ET_{Landsat,i}}} \right\} \quad (7)$$

Where $\overline{ET_{MODIS,i}}$ is the ET mean value of the MODIS maps; $ET_{Landsat,j}$ is the daily ET map of Landsat and $\overline{ET_{Landsat,i}}$ is the ET mean value of Landsat.

The WUE was computed using Equation (8) and expressed in (kg/m^3). The calculation of WUE was based on seasonal ET and yield (Y) which was obtained from Photosynthetically active radiation (PAR). The method was described in detail by Teixeira et al. [23]:

$$WUE = \frac{Y}{ET_s} \quad (8)$$

3. RESULTS AND DISCUSSION

Figure 3 represents the seasonal ET in the semiarid climatic condition of Gezira scheme during the winter season (December 1 through March 15). The pixels of the image include irrigated crops, natural vegetation, wet lands and settlement areas. The ET_s ranges between 30 mm to 717 mm, which reflects the variability of the land cover and quality. The highest ET_s values were found for irrigated crops and wet land spots. Visual analysis and interpretation of Figure 3 showed that groups Hosh, Center, Masalamiya, Wadi Sha'er, North and North West have high ET_s . The value of reference ET_o from Penman_Monteith for the same period was 689 mm. The maximum ET resulted from SEBAL is only 4% higher than Penman_Monteith. This produced a crop coefficient (k_c) value of 1.04, which is somewhat similar to crop coefficient of open water surfaces. The result demonstrates the effectiveness of using satellite-based model to quantify crop water demand in large area.

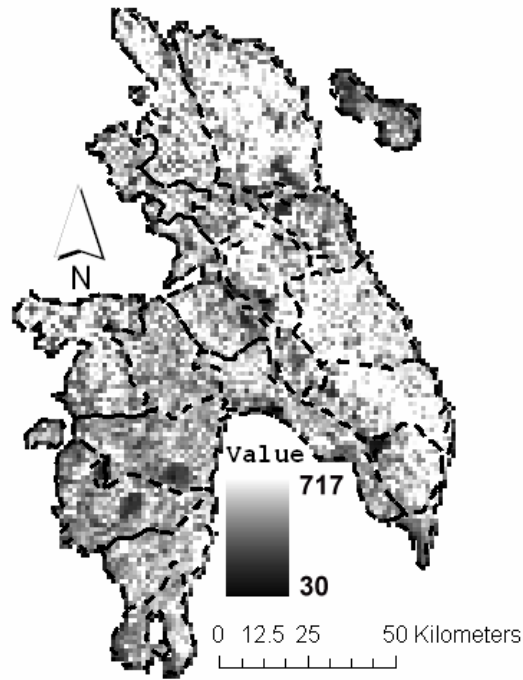


Figure 3. Average ET_s (December 1-March 15) for Gezira scheme (mm)

Figure 4 shows the validation of the retrieved daily ET for wheat at Gezira Research Station (GRS). The ET of crops can be estimated directly from empirical relationships. Various theoretical or empirical approaches commonly use the ET_o-k_c to estimate crop evapotranspiration (ET_c). SEBAL actual ET during the eight overpass days of MODIS was compared with ET_c of wheat obtained by ET_o-k_c method. The results obtained show that the error between SEBAL and ET_c is about 18%, however, much of the error on individual days will randomly distribute and cancel during the seasonal calculation. Our results are consistent with Bastiaanssen et al. [24].

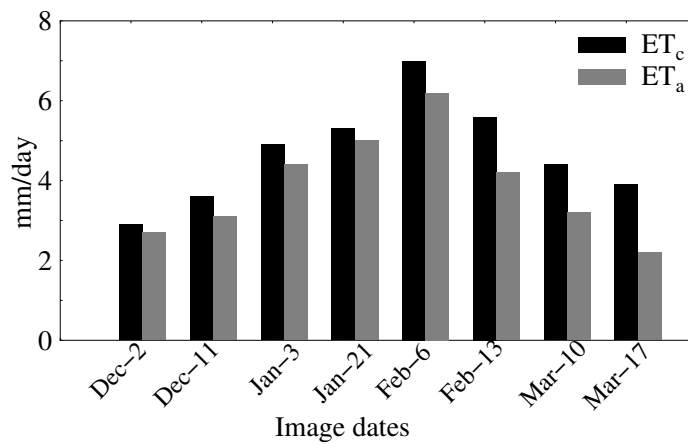


Figure 4. Comparison of actual ET (ET_a) with crop ET (ET_c) of wheat at GRS

Figure 5 shows the evaporative depletion and average seasonal ET for each group of Gezira scheme. Total water depletion for the whole area found to be 2463 million m³, the value within the range reported by Adam [25]. It is also clear that groups South, Eastern, Abu Gota, Wad haboba and Shawal show the lowest water depletion (less than 100 million m³), however, peak water depletion occurs in the North group (329 million m³). The other 12 groups reflect a wide variability due to the amount of beneficial depletion of water resources by wheat and cotton, their depletion value ranges from 100 to 200 million m³. It should be noted that, the current research is the first regional-scale application in the Gezira scheme; hence, information reported here could be useful for decision makers to improve irrigation performance through a fair redistribution and allocation of water resources in time and space. Average seasonal ET_s has similar trend of total water depletion which ranges between 160 mm and 297 mm.

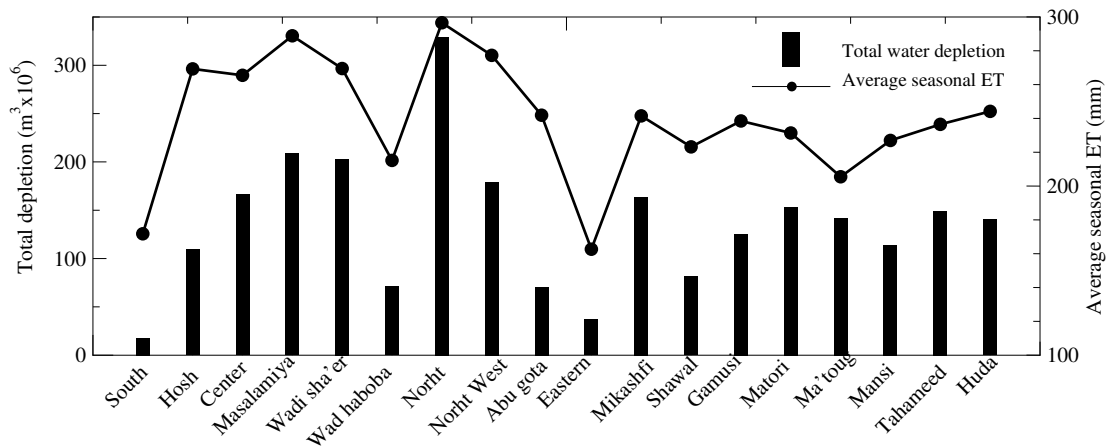


Figure 5. Total water depletion (m³) and average ET_s for different administrative units of Gezira scheme

The statistical calculations of ET_s of wheat at each group are listed in Table 2. During the winter season (December-March), ET_s was higher in Masalamiya and Center, however, ET_s values in groups Wadi Sha'er, Gamusi and Mikashfi were less than 400 mm. other groups show average ranges between 405 mm and 429 mm.

Table 2. Statistical calculation of seasonal ET of wheat at administrative level

Admin. Unit	Min.	Max.	Mean	STDEV	CV%
South	328	487	419	30	7
Hosh	294	524	409	72	12
Center	398	500	449	72	16
Masalamiya	436	563	499	89	18
Wadi Sha'er	274	525	397	79	20
Wad Haboba	247	641	421	84	20
North	251	569	409	70	17
North West	287	546	414	81	20
Abu Gota	331	490	425	84	20
Mikashfi	348	380	360	17	5
Gamusi	314	406	360	66	18
Matori	387	447	426	33	8
Ma'toug	266	573	419	69	17
Mansi	322	558	421	123	29
Tahameed	227	620	405	74	18
Huda	372	531	429	51	12

Average coefficient of variation and standard deviation among all groups is 16% and 68 mm, respectively.

Statistical analyses of water use efficiency of wheat are demonstrated in Table 3. Despite the close mean values among all groups, six groups showed WUE higher than 0.5 kg/m^3 (Center, Wadi Sha'er, North, North West, Mikashfi and Gamusi), which could be due to higher yield obtained. Average variations in WUE were higher (37%) compared with ET_s , which could be contributed to large variations that observed for yield. Average standard deviation of WUE for all groups was 0.161 kg/m^3 .

The calculated statistics of ET_s , yield and WUE for the 18 groups of the Gezira scheme are illustrated in Table 4. Salwa [4] and Fadl [2] derived seasonal ET for wheat using water balance approach, their results ranged between 423 mm and 500 mm which are close to our results given in Table 4.

Table 3. Statistical calculation of on farm WUE of wheat at administrative level

Admin. Unit	Min.	Max.	Mean	STDEV	CV%
South	0.11	0.72	0.48	0.159	33
Hosh	0.03	0.72	0.42	0.136	33
Center	0.22	0.62	0.52	0.142	27
Masalamiya	0.24	0.54	0.37	0.122	33
Wadi Sha'er	0.21	0.88	0.56	0.195	35
Wad Haboba	0.06	1.22	0.43	0.215	50
North	0.05	1.17	0.54	0.210	39
North West	0.13	0.62	0.52	0.107	21
Abu Gota	0.10	0.54	0.37	0.205	55
Mikashfi	0.13	0.71	0.54	0.153	28
Gamusi	0.17	0.72	0.59	0.173	29
Matori	0.12	0.45	0.35	0.105	30
Ma'toug	0.11	0.88	0.42	0.145	35
Mansi	0.14	0.58	0.34	0.225	66
Tahameed	0.11	0.42	0.36	0.089	25
Huda	0.17	0.65	0.42	0.195	46

Various research studies of WUE for wheat in the Gezira scheme reported a range between 0.07 and 0.37 kg/m³. While the current research showed a mean WUE of 0.49 kg/m³, with a range between 0.05 kg/m³ and 1.2 kg/m³. Large variations in WUE were also detected between different farmers field (39% coefficient of variation), these variations were due to yield diversity among farmers field (41%). The range of WUE (0.05 to 1.2 kg/m³) indicates that there is a huge potential to enhance WUE to save water resources in the irrigated scheme of the Gezira.

Table 4. Average calculated statistics of ETs, yield and WUE for wheat in the Gezira scheme

	Minimum	Maximum	Mean	Standard deviation	CV%
ET_s (mm)	251	569	411	70	17
Yield (t/ha)	0.30	4.1	2.0	0.81	41
WUE (kg/m³)	0.05	1.2	0.49	0.19	39

The relationships between seasonal ET_s , WUE and yield are given by Figure 6. It is obvious from Figure 6 that WUE and yield were increased as ET_s increased, then dropped as ET_s continue to increase. It should be noted that ET_s higher than 450 mm gave lower yield and WUE, which shows that much water does not always obtain higher yield.

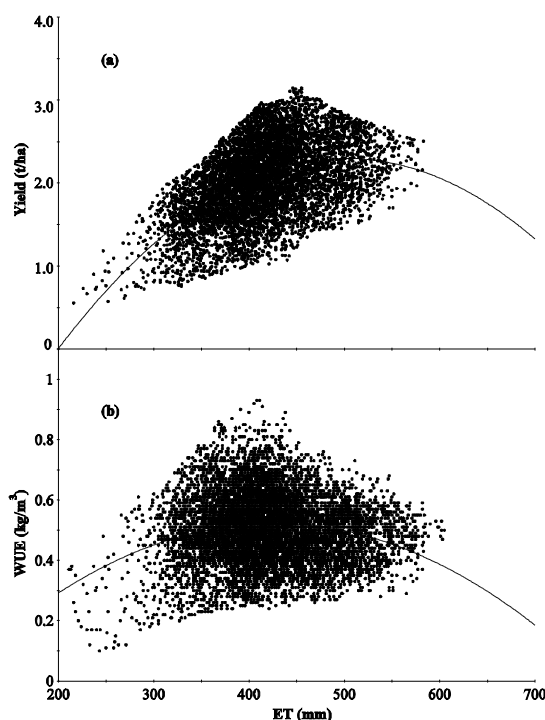


Figure 6. The relationship of ETs versus (a) yield and (b) WUE of wheat

4. CONCLUSION

The study shows that it is possible to use remote sensing data and satellite-based EB model to assess the water depletion and water use efficiency of large irrigated scheme. In this paper SEBAL model was applied to Landsat data and freely available MODIS images to investigate the seasonal water depleted and water use efficiency at administrative level of the Gezira scheme.

The results of the remote sensing analysis show that the Gezira scheme during winter season requires total amount of 2463 million m^3 to fulfill the irrigation needs. A combination of Landsat and MODIS images were used to estimate the seasonal ET which ranges between 30 mm and 717 mm, however, average ET_s for wheat across different groups found to be about 411 mm. In this research the relative percentage errors between estimated and observed ET on daily and seasonal basis are approximately 18% and 4%, respectively. However, coefficient of variation among different administrative units was 16%.

To assess the irrigation performance, WUE was calculated and the relationships among seasonal ET_s and yield of wheat were established. Results showed that WUE and yield were decreased as ET_s increased beyond 450 mm, which indicates that much water are not necessary to obtain higher yield, therefore yield is a key factor to improve WUE. Results also revealed that there is a potential scope to improve yield and WUE in the Gezira scheme.

Acknowledgement

The authors are pleased to acknowledge the full financial support of the Japan Society for the Promotion of Science (JSPS).

REFERENCES

1. Farbrother, H.G., Block inspector guide to the "Advance Indent". Table of crop water requirements of Gezira crops. Second Issue-April, 1973.
2. Fadl, O.A., Evapotranspiration measured by a neutron probe on Sudan Gezira Vertisols, *Experimental Agriculture*, Vol. 14, pp. 341-347.
3. Farah, S.M., Salih, A.A., Taha, A.M., Ali, Z.I. and Ali, I.A., Grain sorghum response to supplementary irrigation under post-rainy season conditions, *Agricultural Water Management*, Vol. 33, part 1, pp. 31-41.
4. Salwa, Y., Irrigation water requirements of two cultivars of wheat under Gezira condition, M.Sc. Thesis, University of Gezira, Sudan, 1997.
5. Abdelhadi, A.W., Hata, T., Tanakamaru, H., Tada, A. and Tarig, M.A., Estimating of crop water requirements in arid region using Penman-Monteith equation with derived crop coefficients: a case study on Acala cotton in Sudan Gezira irrigated scheme, *Agricultural Water Management*, Vol. 45, part 2, pp. 203-214.
6. Abdelhadi, A.W., El Awad, S.E.A., Bashir, M.A. and Hata, T., Evaluation of wheat bed planting system in irrigated Vertisols of Sudan, *Agricultural Mechanization in Asia, Africa, and Latin America*, Vol. 37, part 3, pp. 62-67.
7. Adeeb, A.M., Water productivity of food crops in Gezira scheme, Sudan, *Proceedings of environmentally sound technology in water resources management*, Gaborone, Botswana, 2006.
8. Menenti, M. and Choudhury, B.J., Parameterization of land surface evapotranspiration using a location dependent potential evapotranspiration and surface temperature range, in *Exchange processes at the land surface for a range of space and time scales* (Ed. Bolle, H.J. et al.) pp. 561-568, *International Symposium*, 1993.
9. Bastiaanssen, W.G.M., Regionalization of surface flux densities and moisture indicators in composite terrain: a remote sensing approach under clear skies in Mediterranean climates. Report 109. Agricultural Research Department, Wageningen, The Netherlands, 1995.

10. Kustas, W.P. and Norman, J.M., Use of remote sensing for evapotranspiration monitoring over land surface, *IAHS Hydrological Sciences Journal*, Vol. 41, part 4, pp. 495-516.
11. Roerink, G.L., Su, B. and Menenti, M., S-SEBI A simple remote sensing algorithm to estimate the surface energy balance, *Physics and Chemistry of the Earth (B)*, Vol. 25, part 2, pp. 147-157.
12. Su, Z., The Surface Energy Balance System (SEBS) for estimation of turbulent heat fluxes, *Hydrology and Earth System Sciences*, Vol. 6, part 1, 85-99.
13. Loheide II, S.P. and Gorelick, S.M., A local-scale, high-resolution evapotranspiration mapping algorithm (ETMA) with hydroecological applications at riparian meadow restoration sites, *Remote Sensing of Environment*, Vol. 98, part 2, pp. 182-200.
14. Allen, R.G., Tasumi, M. and Trezza, R., Satellite-based energy balance for mapping evapotranspiration with internalized calibration (METRIC)-model, *Journal of Irrigation and Drainage Engineering ASCE*, Vol. 133, part 4, pp. 380-394.
15. Bastiaanssen, W.G.M., Menenti, M., Feddes, R.A. and Holtslag, A.A.M., A remote sensing surface energy balance algorithm for land (SEBAL): 1. Formulation, *Journal of Hydrology*, Vol. 212-213, part 2, pp. 198-212.
16. Bastiaanssen, W.G.M., SEBAL-based sensible and latent heat fluxes in the irrigated Gediz Basin, Turkey, *Journal of Hydrology*, Vol. 229, part 2, pp. 87-100.
17. Trezza, R., Evapotranspiration using a satellite-based surface energy balance with standardized ground control. Ph.D. Dissertation, Utah State University, Logan, UT., 2002.
18. Mohamed, Y.A., Bastiaanssen, W.G.M. and Savenije, H.H.G., Spatial variability of actual evaporation and soil moisture across the Sudd determined by SEBAL and the impact on monthly water balances, *Journal of Hydrology*, Vol. 289, part 2, pp. 145-164.
19. Farah, H.O., Bastiaanssen, W.G.M. and Feddes, R.A., Evaluation of the temporal variability of the evaporative fraction in a tropical watershed, *Int. J. of Applied Earth Observation and Geoinformation*, Vol. 5, part 2, pp. 129-140.
20. Gao, Y., Long, D. and Zhao-Liang, L., Estimation of daily actual evapotranspiration from remotely sensed data under complex terrain over the upper Chao river basin in North China, *International Journal of Remote Sensing*, Vol. 29, part 11, pp. 3295-3315.
21. Tasumi, M., Bastiaanssen, W.G.M. and Allen, R.G., Application of the SEBAL methodology for estimating consumptive use of water and streamflow depletion in the Bear River Basin of Idaho through remote sensing. Appendix C: A step-by-step guide to running SEBAL. Final report. The Raytheon Systems Company, EOSDIS Project, 2000.
22. Zwart, S.J. and Bastiaanssen, W.G.M., SEBAL for detecting spatial variation of water productivity and scope for improvement in eight irrigated wheat systems, *Agricultural Water Management*, Vol. 89, part 3, pp. 287-296.
23. Teixeira, A.H.C., Bastiaanssen, W.G.M., Ahmed, M.D. and Bos, M.G., Reviewing SEBAL input parameters for assessing evapotranspiration and water

- productivity for the Low-Middle São Francisco River basin, Brazil, *Agricultural and Forest Meteorology*, (In press).
24. Bastiaanssen, W.G.M., Noordman, E.J.M., Pelgrum, H., Davids, G., Thoreson, B.P. and Allen, R.G., SEBAL model with remotely sensed data to improve water-resources management under actual field conditions, *Journal of Irrigation and Drainage Engineering*, Vol. 131, part 1, pp. 85-93.
 25. Adam, H.S., *Agroclimatology, crop water requirements and water management*, Gezira press, Wad Medani, pp. 171, 2005.